

# Sum Frequency Generation Study of the Room-Temperature Ionic Liquids/Quartz Interface

Casey Romero and Steven Baldelli\*

Department of Chemistry, University of Houston, Houston, Texas 77204

Received: November 10, 2005; In Final Form: February 10, 2006

The purpose of this investigation is to study the ionic liquid/quartz interface with sum frequency generation vibrational spectroscopy (SFG). SFG spectroscopy was chosen for this study because of its unique ability to yield vibrational spectra of molecules at an interface. Different polarization combinations are used, which probe different susceptibilities, giving SFG the ability to determine molecular orientation at the interface. The ionic liquids used were 1-butyl-3-methylimidazolium tetrafluoroborate, [BMIM][BF<sub>4</sub>], and 1-butyl-3-methylimidazolium hexafluorophosphate, [BMIM][PF<sub>6</sub>]. To determine the influence of the molecular structure and charge on orientation at the interface, neutral, 1-methylimidazole, and 1-butylimidazole were also studied. Raman spectra and depolarization ratios were obtained for neat samples of 1-methylimidazole, 1-butylimidazole, and 1-butyl-3-methylimidazolium tetrafluoroborate recorded from 2700 to 3300 cm<sup>-1</sup>. SFG spectra of the 1-methylimidazole/quartz interface showed both methyl and aromatic C–H vibrations. Orientation calculations determined that the ring of the molecule is tilted 45–68° from normal, with the methyl group oriented 32–35° from normal. The SFG spectra of 1-butylimidazole contain several resonances from the alkyl chain with only one weak resonance from the aromatic ring. Orientation calculations suggest that the ring is lying in the plane of the surface with the methyl group pointing 43–47° from normal. The orientation of the [BMIM]-[PF<sub>6</sub>] ionic liquid was sensitive to trace amounts of water and had to be evacuated to <3 × 10<sup>-5</sup> Torr for the water to be removed. SFG spectra of both ionic liquids were similar, displaying resonances from the alkyl chain as well as the aromatic ring. Orientation analysis suggests the aromatic ring was tilted 45–90° from normal for [BMIM][BF<sub>4</sub>], while the ring for [BMIM][PF<sub>6</sub>] was tilted 38–58° from normal. This suggests the orientation of the molecule is influenced by the size of the anion.

## Introduction

Room-temperature ionic liquids are a combination of weakly coordinating organic cations and inorganic anions which are liquid at room temperature.<sup>1</sup> Ionic liquids have become a major topic of interest because of their unique properties. They are nonvolatile and nonflammable with a high thermal stability and a low melting point. These qualities allow ionic liquids to be outstanding solvents for many synthesis reactions including biphasic catalysis<sup>2–4</sup> and liquid/liquid extraction.<sup>5,6</sup> Another interesting property of ionic liquids is their ability to be a conductive media for fuel cells and solar cells.<sup>7,8</sup> Recent studies have shown that imidazolium based ionic liquids can be used as lubricants.<sup>9–13</sup> Because most of these applications involve interfacial chemistry it is important to develop a molecular level description of how ionic liquids behave at an interface. There have only been a few studies of the interfacial properties of ionic liquids<sup>14–22</sup> and only one on the ionic liquid/quartz interface.<sup>23</sup> This study's purpose is to investigate the ionic liquid/quartz interface with sum frequency generation vibrational spectroscopy. The ionic liquids used were 1-butyl-3-methylimidazolium tetrafluoroborate, [BMIM][BF<sub>4</sub>], and 1-butyl-3-methylimidazolium hexafluorophosphate, [BMIM][PF<sub>6</sub>]. To determine how shape and charge affected the orientation at the interface, 1-methylimidazole and 1-butylimidazole were also studied. Analysis of SFG data in the determination of orientation requires accurate assignment of observed vibrational modes.

Polarized Raman spectroscopy was used to help with vibrational mode assignment and to determine depolarization ratios of the vibrations.

## Sum Frequency Generation

Sum Frequency Generation (SFG) was used for these experiments because it is insensitive to bulk solvent and will only probe molecules oriented at the interface. SFG spectroscopy is a nonlinear technique used to investigate vibrational resonances of molecules at an interface. With SFG, a tunable infrared laser and a fixed frequency visible laser are overlapped both spatially and temporally at the surface and the emitted light at the sum of the two input fields is detected. As the infrared frequency is scanned to a vibrational resonance of molecules at the interface, the intensity of the emitted beam is increased. More specifically, the intensity of the sum frequency beam depends on the intensities of the incident beams,  $E_{\text{vis}}$  and  $E_{\text{IR}}$ , and the second-order nonlinear susceptibility,  $\chi^{(2)}$ .

$$I_{(\omega_{\text{sum}})} \approx |K_{\text{SFG}} \chi^{(2)} K_{\text{vis}} E_{\text{vis}} K_{\text{IR}} E_{\text{IR}}|^2 \quad (1)$$

$\chi^{(2)}$  is a third-rank tensor and therefore vanishes in bulk media with inversion symmetry. Within the electric dipole approximation, no signal arises from molecules in solution, and is due only to molecules at an interface where the isotropic environment of the bulk phase is broken. The SFG signals from molecules are enhanced when the frequency of the infrared beam,  $\omega_{\text{IR}}$ , is in resonance with a sum frequency active vibrational mode.

$$\chi_{\text{R}}^{(2)} = \frac{A}{\omega_{\text{IR}} - \omega_{\text{q}} + i\Gamma} \quad (2)$$

\* To whom correspondence should be addressed. E-mail: sbaldelli@uh.edu.

where  $A$  is the amplitude of the resonance,  $\omega_q$  is the frequency of the vibration, and  $\Gamma$  is the damping constant. There are other contributions to the sum frequency signal which are not dependent on the infrared frequency, called nonresonant contributions.

$$\chi^{(2)} = \chi_{\text{NR}}^{(2)} + \sum \chi_{\text{R}}^{(2)} \quad (3)$$

These nonresonant contributions are usually from the visible radiation being near a electronic transition and are independent of infrared frequency. At metal surfaces  $\chi_{\text{NR}}^{(2)}$  can be comparable to  $\chi_{\text{R}}^{(2)}$ . For monolayers on quartz  $\chi_{\text{NR}}^{(2)}$  is small but cannot be ignored. The resonant portion of  $\chi^{(2)}$  can be related to the hyperpolarizability of the individual molecules in the monolayer,  $\beta$ , by

$$\chi_{\text{R}}^{(2)} = N\langle\beta\rangle \quad (4)$$

$N$  is the number of molecules contributing to the signal and  $\langle\beta\rangle$  is the molecular hyperpolarizability orientationally averaged. The hyperpolarizability is a product of the Raman polarizability,  $\alpha$ , and the transition dipole moment of the molecule,  $\mu$ , and therefore all resonances in SFG spectroscopy must be both infrared and Raman active.

$$\beta_{abc} = \langle g|\alpha_{ab}|v\rangle\langle v|\mu_c|g\rangle \quad (5)$$

The lowercase letters ( $abc$ ) refer to the molecular coordinates which must be transformed to a laboratory fixed coordinate system ( $xyz$ ) using the Euler matrix.

$$\chi_{XYZ} = \sum_{xyz} U_{XYZ}\chi_{xyz} \quad (6)$$

The components of the transformation matrix depend on the Euler angles ( $\theta, \phi, \chi$ ), which relates the molecular and laboratory-fixed coordinate systems. The tilt angle,  $\theta$ , is defined as  $0^\circ$  normal to the surface and  $90^\circ$  in the plane of the surface. The twist angle,  $\phi$ , is defined at  $0^\circ$  in plane with the surface and  $90^\circ$  perpendicular to the surface.  $\chi$  is the azimuthal angle within the plane of the surface.

This paper will be concerned with the stretching modes of the methyl group and the ring modes of the imidazole or imidazolium ring. The methyl group is assumed to have  $C_{3v}$  symmetry with free rotation along the  $C_3$  axis. The molecular coordinate system for the methyl group is defined with the  $z$  axis along the  $C_3$  axis. From group theory we are able to determine which components of the hyperpolarizability tensor are allowed for each vibration. Therefore, the methyl groups ( $C_{3v}$ ) are assumed to have  $\beta_{aac}$ ,  $\beta_{bbc}$ , and  $\beta_{ccc}$  as the hyperpolarizability tensor elements of symmetric stretching modes and  $\beta_{aca}$ ,  $\beta_{bcb}$ ,  $\beta_{caa}$ , and  $\beta_{cbb}$  as hyperpolarizability tensor elements of the antisymmetric modes. The other tensor elements ascribed to the antisymmetric vibrations integrate to zero when free rotation of the methyl group is assumed. This allows the components of the transformation matrix to be averaged over  $\phi$  and  $\chi$ , which leads to an equation that is only a function of the tilt angle  $\theta$ . The other vibrations of concern are the H-C(4)C(5)-H ring modes of the imidazole/imidazolium ring. The molecular coordinate system is defined with the  $z$ -axis along the  $C_2$  symmetry plane of the ring. This vibration is assumed to have  $C_{2v}$  symmetry with  $\beta_{aac}$  and  $\beta_{ccc}$  as the symmetric components of the hyperpolarizability tensor. For the asymmetric modes only  $\beta_{caa}$  and  $\beta_{aca}$  contribute. Since free rotation cannot be assumed for the ring modes, the Euler matrix can

only be integrated in terms of  $\chi$ , and the resulting equation is both a function of tilt  $\theta$  and twist  $\phi$  of the ring mode. Therefore, the results described later are both a function of tilt and twist of the ring vibrations and cannot be separated.

To relate SFG intensity directly to  $\chi^{(2)}$ , the macroscopic local-field corrections, also known as Fresnel coefficients, for the incident fields and for the sum frequency field created at the interface must be calculated. The local-field factors take into account the reflection, refraction, and enhancement of the fields due to the presence of the interface. The local field factors,  $K_{xx}$ ,  $K_{yy}$ , and  $K_{zz}$ , relating to the input visible and infrared electric fields and output sum frequency field, are as follows:<sup>24</sup>

$$K_{xx} = \frac{E_{\text{surface}}}{E_{\text{laser}}}\Big|_x = \frac{2n_1(\omega) \cos\theta_2}{n_2(\omega) \cos\theta_1 + n_1(\omega) \cos\theta_2} \cos\theta_1 \quad (7)$$

$$K_{yy} = \frac{E_{\text{surface}}}{E_{\text{laser}}}\Big|_y = \frac{2n_1(\omega) \cos\theta_1}{n_1(\omega) \cos\theta_1 + n_2(\omega) \cos\theta_2} \quad (8)$$

$$K_{zz} = \frac{E_{\text{surface}}}{E_{\text{laser}}}\Big|_z = \frac{2n_2(\omega) \cos\theta_1}{[n_2(\omega) \cos\theta_1 + n_1(\omega) \cos\theta_2]} \frac{n_1^2(\omega)}{n_m^2(\omega)} \sin\theta_1 \quad (9)$$

where  $\theta_1$  is the incident angle and  $\theta_2$  is the transmitted angle through the media.  $n_1$ ,  $n_2$ , and  $n_m$  are the refractive index of media 1, 2 and the monolayer, respectively. The refractive indices are wavelength dependent and must be determined for both input and the output beams. P-polarized light has contributions in two directions,  $x$  and  $z$ . Therefore,  $K_{xx}$  and  $K_{zz}$  are the two components of p-polarized light once they have been separated. This is accounted for by the  $\cos\theta_1$  and  $\sin\theta_1$  at the end of the respective equations.  $n_1^2/n_m^2$  has been added to  $K_{zz}$  to make corrections due to the polarization sheet of the interface.<sup>25</sup> The refractive index of a material is a macroscopic property, which has led to much debate about how to calculate the refractive index of the monolayer,  $n_m$ .<sup>26,27</sup> The sign of the Fresnel factors comes directly from the coordinate system used for the calculation. The coordinate system used in this study has the  $z$ -coordinate pointing down into the interface.<sup>24,28</sup> This causes all the  $z$ -components of the electric field vectors to be negative. The  $x$ -coordinate is pointing away from the incident beams, therefore the incident electric fields have negative  $x$ -components and the output electric field has a positive  $x$ -component. The sign of the Fresnel coefficients is important for calculating the relative sign of each susceptibility tensor in the ppp polarization combination due to the different tensor elements interfering with one another.

Monolayers that are isotropic in the plane of the surface only have four independent components of  $\chi_{ijk}^{(2)}$ .  $\chi_{zxx}^{(2)} = \chi_{zyy}^{(2)}$ ,  $\chi_{zxx}^{(2)} = \chi_{zyy}^{(2)}$ ,  $\chi_{xxz}^{(2)} = \chi_{yyz}^{(2)}$  and  $\chi_{zzz}^{(2)}$ . Only four combinations of polarization allow sum frequency emission: ssp (s-polarized sum frequency output, s-polarized visible input, p-polarized infrared input), ppp, sps, and pss. Each of these polarization combinations probes a different tensor element of  $\chi_{ijk}^{(2)}$ , except for the ppp combination, which probes a combination of tensor elements.

$$I_{\text{ssp}} \approx |K_{\text{sfg}}^y \chi_{yyz}^{(2)} K_{\text{vis}}^y K_{\text{IR}}^z|^2 \quad (10)$$

$$I_{\text{sps}} \approx |K_{\text{sfg}}^y \chi_{yyz}^{(2)} K_{\text{vis}}^z K_{\text{IR}}^y|^2 \quad (11)$$

$$I_{\text{pss}} \approx |K_{\text{sfg}}^z \chi_{zyy}^{(2)} K_{\text{vis}}^y K_{\text{IR}}^y|^2 \quad (12)$$

$$I_{\text{ppp}} \approx |K_{\text{sfg}}^z \chi_{zzz}^{(2)} K_{\text{vis}}^z K_{\text{IR}}^z + K_{\text{sfg}}^z \chi_{zxx}^{(2)} K_{\text{vis}}^x K_{\text{IR}}^x + K_{\text{sfg}}^x \chi_{xzz}^{(2)} K_{\text{vis}}^z K_{\text{IR}}^x + K_{\text{sfg}}^x \chi_{xxz}^{(2)} K_{\text{vis}}^x K_{\text{IR}}^z|^2 \quad (13)$$

By using the vibrational frequencies and intensities, the type and amount of the adsorbed species can be determined. The orientation of molecules at the interface can be determined by analyzing different polarization combinations of the incident beams.

### Polarized Raman Spectroscopy

Molecular spectroscopy is used to obtain information about the structure and properties of molecules from their vibrational transitions. Raman scattering is a two-photon event in which the incoming radiation creates an induced dipole moment in the molecule. The light emitted by the induced dipole moment is shifted in frequency from the incident radiation by the vibrational energy that is gained or lost due to a vibrational transition of the molecule. When plane polarized electromagnetic radiation is scattered from a molecule there is often a change in the state of polarization.<sup>29</sup> These changes in polarization can be correlated with the symmetry of the molecule. This effect is taken advantage of with polarized Raman spectroscopy. Raman spectroscopy is an inelastic light scattering technique that probes transitions between different vibrational energy levels in a molecule. By probing a system with linearly polarized light and then collecting both the parallel and perpendicular components of the scattered light separately, the amount of intensity of the two spectra can be compared.

$$\rho = \frac{I_{\perp}}{I_{\parallel}} \quad (14)$$

The depolarization ratio,  $\rho$ , is the intensity of the perpendicular component of a vibration,  $I_{\perp}$ , divided by the parallel component,  $I_{\parallel}$ .<sup>30</sup> Depolarization ratios as defined above usually have a value between 0 and 1. If the depolarization ratio is 0 then the scattered radiation is completely polarized and if the depolarization ratio is 1 then the scattered radiation is completely natural.<sup>29</sup> Because of this effect polarized Raman spectroscopy has the ability to probe vibrational modes and determine if they are symmetric or asymmetric modes. This allows for more precision in the assignment of vibrational modes by narrowing down the possible assignments due to its symmetry.

### Experimental Section

**Raman Spectroscopy.** Polarized Raman spectra were acquired with a standard scanning Raman spectrometer.<sup>29,31,32</sup> The spectrometer used a Spex 1403 double monochromator equipped with two 1800 grooves/mm gratings and a Hamamatsu 928 photomultiplier tube. A Coherent Innova 90-6 Ar<sup>+</sup> ion laser with an output power of 50 mW provided the 514.5 nm excitation wavelength. Samples were sealed in NMR tubes and analyzed, in a backscattering geometry, over the CH stretching region, 2700–3300 cm<sup>-1</sup>. Spectra were obtained with a polarization filter parallel to the plane of incidence, the parallel component, and with the polarization filter perpendicular to the plane of incidence, the perpendicular component, for 1-methylimidazole, 1-butylimidazole, and 1-butyl-3-methylimidazolium tetrafluoroborate.

**SFG Optical Setup.** The details of the homemade SFG spectrometer used have been described elsewhere.<sup>15</sup> The laser used to create the fundamental beam was a picosecond pulsed Nd:YAG (Ekspla) with a 20 Hz repetition rate. The fundamental (1064 nm) is used to pump an optical parametric generator (LaserVision) to create a frequency doubled fixed visible beam (532 nm) and a tunable infrared beam between 2000 and 4000 cm<sup>-1</sup>. The optical geometry used was a co-propagating con-

figuration with incident angles of 50° and 60° for the visible and infrared beams, respectively. The fixed visible and tunable infrared beams were sent through polarizers and half waveplates to control the energy and polarization of the incident beams and overlapped both spatially and temporally at the surface of the sample. The SFG signal created at the surface was filtered from the incident visible beam by optical filters, sent through a monochromator, detected by a photomultiplier tube, and analyzed by a gated integrator. A computer program created in LabVIEW was used to collect the signal from the gated integrator and to scan the infrared frequency. The infrared frequency was scanned at 1 cm<sup>-1</sup>/s. Data presented here are an average of five scans of the infrared frequency over the desired range.

**Sample Preparation.** 1-Butyl-3-methylimidazolium tetrafluoroborate and 1-butyl-3-methylimidazolium hexafluorophosphate were synthesized in lab by a procedure detailed in ref 16. 1-Methylimidazole and 1-butylimidazole were purchased from Aldrich and used without further purification. A SFG spectrum was acquired for a distilled sample of 1-butylimidazole and looked identical to spectra taken without distillation. The cell used for these experiments was made entirely out of glass with a Teflon encapsulated silicon O-ring between the cell and the equilateral IR quartz prism (ISP optics) used as the window. This allowed for the entire cell to be cleaned with a 50/50 nitric/sulfuric acid solution. The cell was then rinsed repeatedly with water from a Millipore A10 system (>18 M $\Omega$ ·cm<sup>2</sup>) and dried with flowing nitrogen before being filled with the compound of interest. [BMIM][PF<sub>6</sub>] was sensitive to trace amounts of water and had to be pumped down to <3 × 10<sup>-5</sup> Torr and backfilled with argon gas to remove contributions due to water from the spectra. [BMIM][BF<sub>4</sub>] did not seem to be as sensitive to minute amounts of water, but was also pumped down to <3 × 10<sup>-5</sup> Torr for comparison with [BMIM][PF<sub>6</sub>]. Originally an IR quartz window was used for the experiments but the signal level was very weak. The use of an equilateral quartz prism drastically increased the amount of signal detected. This will be discussed in detail in the results section.

### Results

**Raman Spectroscopy.** Raman spectra and depolarization ratios were obtained for a neat sample of 1-methylimidazole, 1-butylimidazole, and 1-butyl-3-methylimidazolium tetrafluoroborate. Polarized Raman spectra of [BMIM][PF<sub>6</sub>] are not shown because the cation is the same as [BMIM][BF<sub>4</sub>] and the anions were not probed in the region of this study. Spectra were recorded from 2700 to 3300 cm<sup>-1</sup> and are presented in Figures 1, 2, and 3, respectively. For each of the Raman spectra, A is the parallel component and B is the perpendicular component. These data along with calculated depolarization ratios are summarized in Tables 1, 2, and 3, respectively. Spectra were fit by using multiple Lorentzian line shapes with Origin 6.0 software. Line widths and peak assignments were held constant for both perpendicular and parallel components, while only varying the amplitude.

**1-Methylimidazole.** There have been many studies on the vibrational structure of imidazole,<sup>33–37</sup> but only a few studies have been performed on 1-methylimidazole.<sup>38,39</sup> For 1-methylimidazole (Figure 1) eight vibrations were fitted for both the parallel and perpendicular spectra. These vibrations are all due to CH stretches from the methyl group and the ring. The peak assignments and the results of the other two studies of 1-methylimidazole are also summarized in Table 1. Depolarization ratios (also shown in Table 1) correlated well with values reported by Pemberton<sup>38</sup> and made assignments of the vibrations

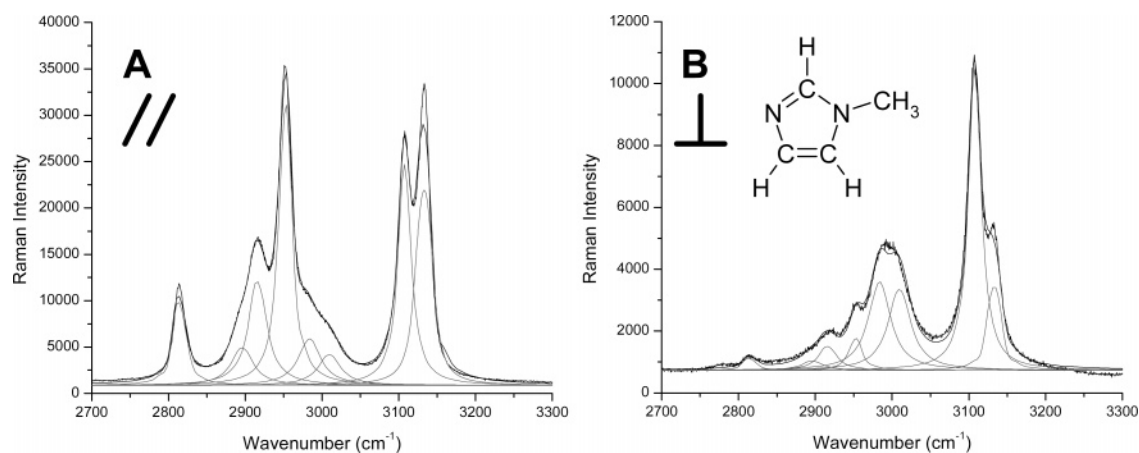


**Figure 1.** Polarized Raman spectra of 1-methylimidazole: (A) parallel component (B) perpendicular component.

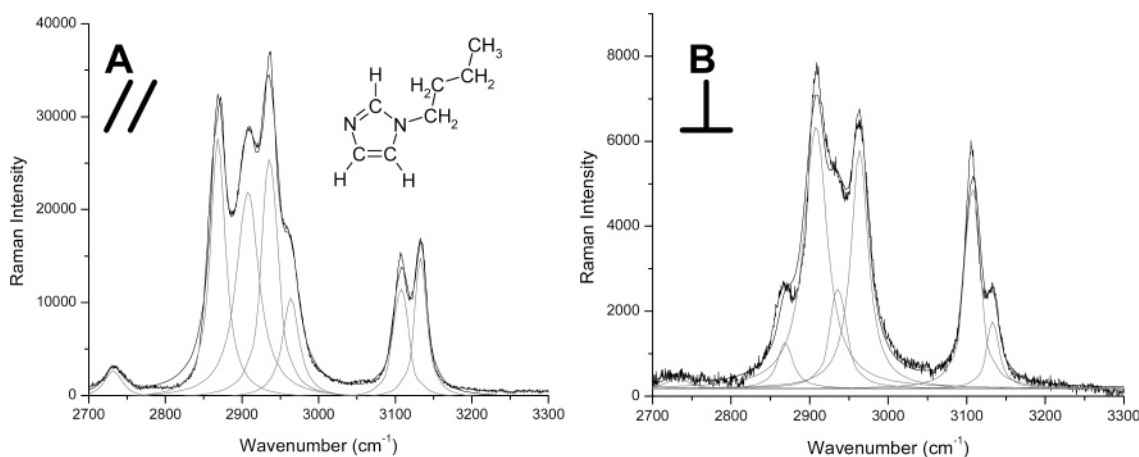


**Figure 2.** Polarized Raman spectra of 1-butylimidazole: (A) parallel component (B) perpendicular component.

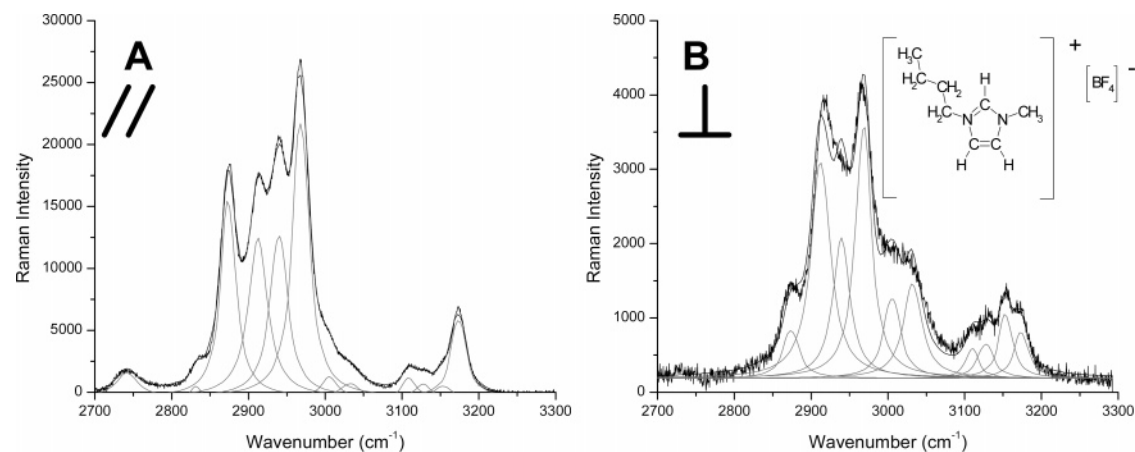


**Figure 3.** Polarized Raman spectra of 1-butyl-3-methylimidazolium  $[\text{BF}_4]^-$ : (A) parallel component (B) perpendicular component.

more accurate. Three vibrations have been assigned to stretches due to the methyl group. The vibrations at 2916, 2952, and 2984  $\text{cm}^{-1}$  are from the Fermi resonance, the symmetric, and the antisymmetric modes, respectively, whereas Pemberton assigns the Fermi resonance as the symmetric mode with the higher frequency. The Fermi resonance is an overtone of the antisymmetric bending mode of the methyl group at 1475  $\text{cm}^{-1}$ .<sup>38</sup> The difference in assignment from Pemberton et al. of the Fermi resonance and symmetric stretching mode is because the Fermi resonance vibration cannot have more intensity than the fundamental.<sup>40</sup> When an overtone has exactly the same vibrational frequency as a normal mode the maximum energy that can be transferred is half the normal modes intensity. When an

**TABLE 1: Vibrational Assignments and Depolarization Ratios of 1-Methylimidazole**

ref 39	ref 38	Raman exptl	vibrational assignment	$\rho$	
				ref 38	exptl
	2822	2814	combination band	0.01	0.04
	2896	2896		0.01	0.07
	2967	2916	sym (CH <sub>3</sub> ) FR	0.03	0.07
2952	2932	2952	sym (CH <sub>3</sub> )	0.01	0.03
	2995			0.06	
3016	3010	2984	asym (CH <sub>3</sub> )	0.66	0.57
	3032	3010	(CH) C2 ring	0.47	0.79
3105	3126	3108	asym (CH) ring	0.41	0.41
3131	3149	3133	sym (CH) ring	0.1	0.11

**TABLE 2: Vibrational Assignments and Depolarization Ratios of 1-Butylimidazole**

Raman exptl	vibrational assignment	$\rho$ exptl
2732	combination band	0.09
2869	sym (CH <sub>3</sub> )	0.04
2907	asym (CH <sub>2</sub> )	0.27
2936	sym (CH <sub>3</sub> ) FR	0.09
2964	asym (CH <sub>3</sub> )	0.52
3107	asym (CH) ring	0.40
3133	sym (CH) ring	0.10

**TABLE 3: Vibrational Assignments and Depolarization Ratios of [BMIM][BF<sub>4</sub>]**

Raman exptl	vibrational assignment	$\rho$ exptl
2742	combination band	<0.01
2833	sym (CH <sub>2</sub> )	<0.01
2874	sym (CH <sub>3</sub> )	0.04
2912	asym (CH <sub>2</sub> )	0.23
2939	sym (CH <sub>3</sub> ) FR	0.13
2968	asym (CH <sub>3</sub> ), sym N-CH <sub>3</sub>	0.14
3005-3035	asym N-CH <sub>3</sub>	0.69
3032	H-bonding interaction	1.13
3109		0.25
3127	(CH) C2 ring	0.46
3153	asym (CH) ring	0.89
3174	sym (CH) ring	0.09

overtone is not exactly overlapped with the fundamental the energy transferred is less than half. Therefore, the fundamental mode must have more intensity than the Fermi resonance.

There are three vibrations that are from the ring modes. The peak at 3010 cm<sup>-1</sup> has been assigned to the CH stretch of the C2 position. The peaks at 3108 and 3133 cm<sup>-1</sup> are assigned to the antisymmetric and symmetric H-C(4)C(5)-H vibrations, respectively. The peak at 2814 cm<sup>-1</sup> has been assigned as a combination band by Pemberton,<sup>38</sup> while the vibration at 2896 cm<sup>-1</sup> has been reported by Pemberton but is unassigned.

**1-Butylimidazole.** There have been no studies of the Raman spectra of 1-butylimidazole listed in the literature, therefore peak assignments were based on imidazole and 1-methylimidazole<sup>33,38,39</sup> for the ring modes and long alkyl chains<sup>41,42</sup> were used to assign the butyl chain vibrations. Depolarization ratios also helped determine assignments by defining the vibration as either symmetric or antisymmetric. The Raman spectra were fit with seven peaks. The peaks at 2869, 2936, and 2964 cm<sup>-1</sup> were assigned as the symmetric, Fermi resonance, and antisymmetric methyl stretches, respectively. The vibration at 2907 cm<sup>-1</sup> was assigned to the asymmetric methylene stretch. The symmetric methylene stretch which should be near 2850 cm<sup>-1</sup> was not visible in the spectra. For the imidazole ring, the antisymmetric and symmetric H-C(4)C(5)-H vibrations are assigned to the peaks at 3107 and 3133 cm<sup>-1</sup>. The frequencies for the symmetric and antisymmetric stretches from the imidazole ring are the same for 1-methylimidazole and 1-butylimidazole. The CH stretch from the C2 position on the ring was not visible in the spectra.

**1-Butyl-3-methylimidazolium BF<sub>4</sub>.** Polarized Raman spectra of [BMIM][BF<sub>4</sub>] are shown in Figure 3. The spectra were fit with 12 peaks. Spectra of 1-butyl-3-methylimidazolium are more complex than those of 1-methylimidazole or 1-butylimidazole. There are two methyl groups which are in different environments causing them to have different vibrational frequencies. The addition of the charge to the ring shifts the vibrational frequency compared to imidazole, which causes peak assignment to be more difficult. The methyl group at the end of the butyl chain

does not seem to be affected by the charge because of the remoteness from the ring. The vibrational assignments for the symmetric, Fermi resonance, and asymmetric vibrations from the methyl group at the end of the butyl chain are 2874, 2939, and 2968 cm<sup>-1</sup>, respectively. For the methylene groups on the butyl chain the symmetric and asymmetric modes have been assigned to 2833 and 2912 cm<sup>-1</sup>.

Assignments for the methyl group attached to the nitrogen were difficult to assign from the depolarized Raman spectra. Other studies<sup>23,43</sup> show differences in assignment of the N-CH<sub>3</sub> vibrations, therefore, IR and Raman spectra of deuterated [BMIM][PF<sub>6</sub>] were required to assign the symmetric and asymmetric N-CH<sub>3</sub> vibrations at 2968 and 3035 cm<sup>-1</sup>.<sup>44</sup> The assignment of both the N-CH<sub>3</sub> symmetric mode and the asymmetric methyl stretch from the butyl chain at 2968 cm<sup>-1</sup> explains the depolarization ratio being 0.14, due to overlapping of the two vibrational modes. The asymmetric N-CH<sub>3</sub> is assigned at 3005-3035 cm<sup>-1</sup> in the polarized Raman spectra, due to a low cross-section. There are three assignments made for modes attributed to the ring, the asymmetric and symmetric H-C(4)C(5)-H vibrations of the ring at 3153 and 3174 cm<sup>-1</sup>, respectively, and the vibration from the C2 CH stretch at 3127 cm<sup>-1</sup>. There is also a hydrogen bonding interaction at 3032 cm<sup>-1</sup> that is discussed by Wilkes et al.<sup>45</sup> The other peaks in the spectra at 2742 and 3109 cm<sup>-1</sup> are not assigned but could be vibrations from the methyl attached to the nitrogen, combination, or overtone vibrations.

**SFG Spectroscopy.** SFG spectra were first performed with use of a quartz window instead of the equilateral prism. This produced spectra with a small amount of signal due to the Fresnel factors at the surface. Because the Fresnel factors are dependent on the refractive index of the media as well as the incident angle, by changing the incident angle the amount of signal was increased. The SFG spectrometer setup used has incident angles of 50° and 60° for the visible and infrared beams, respectively. When the beams are sent through a flat quartz window they are refracted and then the incident angles at the interface are 31° and 36° for the visible and infrared, respectively. This change in the angles decreases the local fields at the surface by 50%. Because there are two incident fields (visible and infrared) and the SFG intensity is due to the square of the incident electric fields, the overall SFG intensity is 1/16th of the intensity without a window, see eq 1. This is corrected with an equilateral quartz prism. The prism allows the incident beams to overlap at the interface without changing the angle of the infrared beams and only slightly changing the incident angle of the visible beam (~3°), thus greatly increasing the signal level. The use of a prism allows the incident electric fields to be closer to, but not at, a total internal reflection geometry that has been shown to greatly enhance SFG signal.<sup>46</sup>

SFG spectroscopy was performed on the four compounds of interest with use of four polarization combinations ssp, ppp, sps, and pss from 2750 to 3300 cm<sup>-1</sup>. Only the ssp and ppp spectra are shown because of the weak signal level observed in the other two polarization combinations.

**1-Methylimidazole.** SFG spectra of the 1-methylimidazole/quartz interface are shown in Figure 4. The spectrum on the left is the ssp polarized spectrum and that on the right is the ppp polarized spectrum. Both spectra were fit with six peaks using eq 2 (solid black line). The resonances at 2920, 2962, and 2997 cm<sup>-1</sup> have been assigned to the Fermi resonance, symmetric, and asymmetric methyl stretches, respectively. The vibration at 3060 cm<sup>-1</sup> is due to the CH vibration of the C2 carbon of the imidazole ring. The large change in frequency of

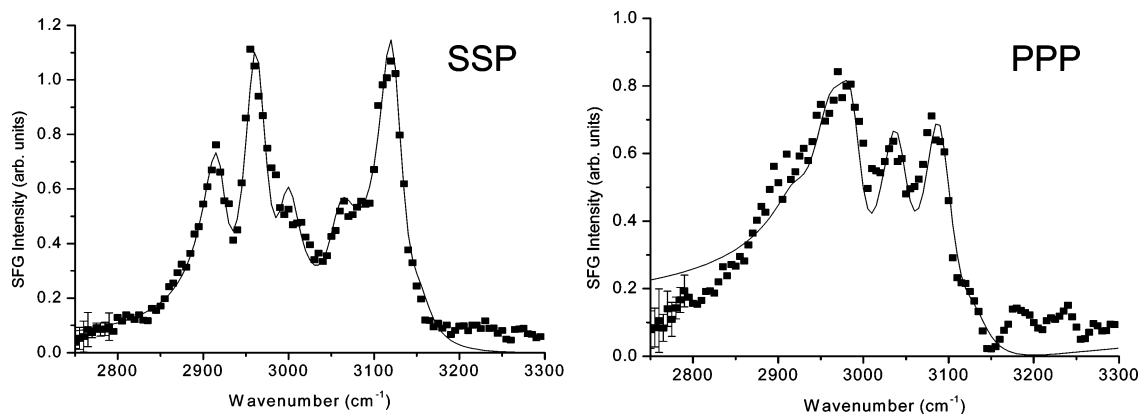


Figure 4. SFG spectra of 1-methylimidazole/quartz interface w/fit.

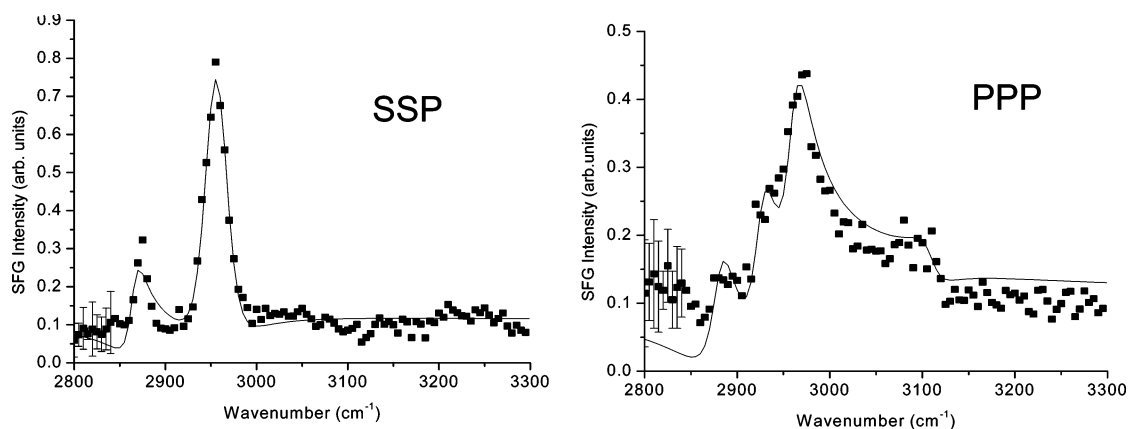


Figure 5. SFG spectra of 1-butylimidazole/quartz interface w/fit.

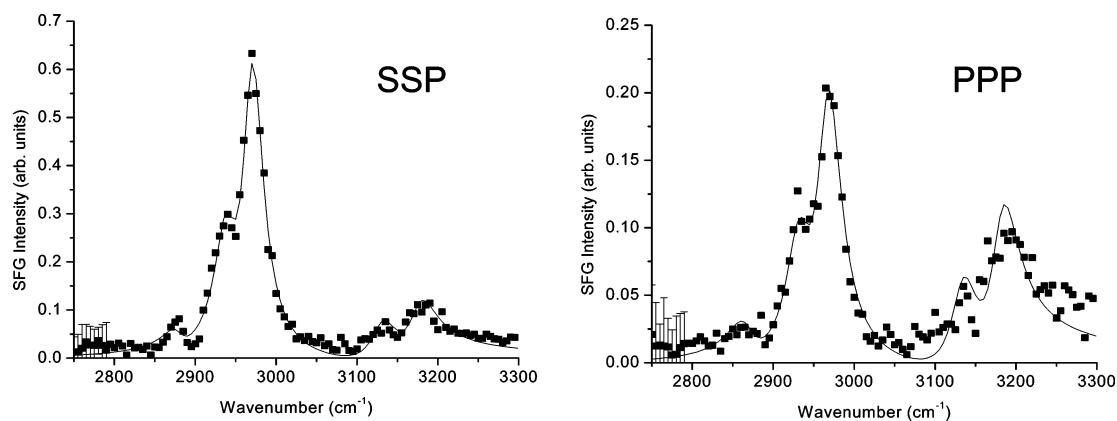


Figure 6. SFG spectra of 1-butyl-3-methylimidazolium [BF<sub>4</sub>]<sup>-</sup>/quartz interface w/fit.

this vibration has been attributed to interaction with the quartz surface because of its acidic nature.<sup>47,48</sup> The vibrations at 3123 and 3152  $\text{cm}^{-1}$  are from the asymmetric and symmetric H-C(4)C(5)-H stretches from the imidazole ring.

**1-Butylimidazole.** The SFG spectra of the 1-butylimidazole/quartz interface are shown in Figure 5. These spectra were drastically different from the 1-methylimidazole. The ssp spectrum was fit with three peaks at 2865, 2947, and 2965  $\text{cm}^{-1}$  assigned symmetric, Fermi resonance, and asymmetric modes from the methyl group. There are no resonances from the imidazole ring in the ssp spectra. The ppp spectra was fit to four peaks corresponding to the same modes for the methyl group and an extra mode at 3110  $\text{cm}^{-1}$  from the asymmetric ring mode from the H-C(4)C(5)-H stretch.

**1-Butyl-3-methylimidazolium Tetrafluoroborate.** SFG spectra of the [BMIM][BF<sub>4</sub>]/quartz interface are shown in Figure

6. Each spectrum was fit with five peaks. Three resonances are from the methyl group at the end of the butyl chain: 2878, 2940, and 2970  $\text{cm}^{-1}$ , which correspond to the symmetric, Fermi resonance, and asymmetric modes, respectively. There are perhaps some other contributions; the fit of the Fermi resonance peak has a much larger amplitude than the fundamental, but has proven difficult to de-convolute. The vibrations from the imidazolium ring are much more straightforward. There are two vibrations in each spectrum at 3130 and 3175  $\text{cm}^{-1}$ , the C-H stretch from the C2 position and the symmetric H-C(4)C(5)-H stretch, respectively.

**1-Butyl-3-methylimidazolium Hexafluorophosphate.** The SFG spectra of the [BMIM][PF<sub>6</sub>]/quartz interface are similar to the [BMIM][BF<sub>4</sub>] spectra. The alkyl portion of the spectra was fit to the same number of peaks as the [BMIM][BF<sub>4</sub>] spectra with vibrations at 2879, 2937, and 2970  $\text{cm}^{-1}$  due to the

TABLE 4: Fresnel Coefficients

	$K_{xx}$	$K_{yy}$	$K_{zz}$
IR	-0.521	0.898	-0.735
visible	-0.605	0.966	-0.755
SFG	0.592	0.965	-0.762

symmetric, Fermi resonance, and asymmetric modes of the methyl group at the end of the butyl chain. There are other modes within this region but because the spectra fit so well with 3 peaks it is difficult to determine how much of the amplitude is due to other vibrations from the methylene groups and the methyl group attached to the nitrogen. There is only one vibration that is attributed to the imidazolium ring at 3180  $\text{cm}^{-1}$ , which is the symmetric H-C(4)C(5)-H stretch.

## Discussion

**Orientation Calculation.** A detailed description of the orientation calculation for the solid/liquid interface of 1-methylimidazole/quartz, 1-butylimidazole/quartz, and the two ionic liquids is described below. Indices of refraction used in calculating the Fresnel coefficients are wavelength dependent. For the quartz prism, 1.46 was used as the refractive index for the visible and SFG wavelength,<sup>49</sup> and 1.41 for the infrared wavelength. Values for the refractive index of the four molecules studied at the different input and output wavelengths were not available. Ouchi et al.<sup>14</sup> used a value of 1.41 (532 nm) and 1.37 (3.0  $\mu\text{m}$ ) for the refractive index of [BMIM][BF<sub>4</sub>] and [BMIM][PF<sub>6</sub>], but does not state a value for the sum frequency refractive index. The refractive index of 1-methylimidazole, 1.497,<sup>50</sup> was used for all compounds and all wavelengths. This allows for a more systematic comparison of the four compounds without increasing the error significantly. The refractive index of 1-methylimidazole was also used for  $n_m$  to make corrections due to the polarization sheet. Using the bulk refractive index is a common way of ascribing a value to the refractive index of the monolayer,<sup>51</sup> and is close to the refractive index of the monolayer ( $\sqrt{2}$ ) used by Bain.<sup>27,52</sup> The optical Fresnel coefficients calculated with eqs 7, 8, and 9 are listed in Table 4. These values were used for the orientation calculation of all molecules studied. Calculation of the hyperpolarizability tensors for the methyl and ring stretching modes were performed by using the bond additivity model outlined by Hirose et al.<sup>53-55</sup> For  $C_{3v}$  symmetry, the symmetric modes are  $\beta_{aac} = \beta_{bbc} = 4\beta_{ccc}$  and for the antisymmetric modes  $\beta_{caa} = 1.052\beta_{aac}$ . For  $C_{2v}$  symmetry, the symmetric modes are  $\beta_{ccc} = (1/3)\beta_{aac}$ , and for the antisymmetric modes  $\beta_{caa} = 1.06\beta_{aac}$ .

**Peak Fitting and Error Analysis.** Each SFG spectra shown was fit by using eq 3 with an instrumental weighting method that took into account scatter in the data as well as fitting error. The amplitudes and widths of each of the vibrations used for orientation analysis are listed in Table 5. The coefficients given from each of the fits have a standard deviation associated with them. To correctly determine how much effect the error of each coefficient has on the orientation calculation a rigorous error

analysis must be performed. Each peak has three coefficients,  $A$ , the amplitude of the peak,  $\Gamma$ , the damping constant (or width of the peak), and,  $\omega_q$ , which is the frequency of the peak. To correctly compare the intensities of resonances, the amplitudes of each peak were divided by their widths (normalized) and squared.<sup>56,57</sup>

$$I = \left(\frac{A}{\Gamma}\right)^2 \quad (15)$$

When performing mathematical operations on values with a standard deviation a more detailed mathematical operation must be performed.<sup>58</sup> This causes an increase in the percent error, especially the squaring of the term in eq 15.

Another effect that must be taken into account before comparing the intensity ratios from different polarization combinations is the instrumental corrections from the differences in the efficiency of the optics used in the SFG setup for s and p polarized light. The influence of the monochromator is the largest contributor. This effect can be calculated and is treated as a weighting factor, which is multiplied to the intensity to correct for these differences.

The Fermi resonance must be taken into account when comparing the intensity ratios of the methyl stretches of the studied molecules. The Fermi resonance is an overtone vibration, with very low probability, and all of the intensity attributed to it is considered "stolen" from the fundamental symmetric methyl stretch. When comparing the symmetric methyl stretch intensity to an antisymmetric stretch, the amplitude from the Fermi resonance ( $A_{fr}$ ) must be added to the symmetric stretching ( $A_s$ ) amplitude as shown in eq 16.

$$I = \left(\frac{A_s}{\Gamma_s} + \frac{A_{fr}}{\Gamma_{fr}}\right)^2 \quad (16)$$

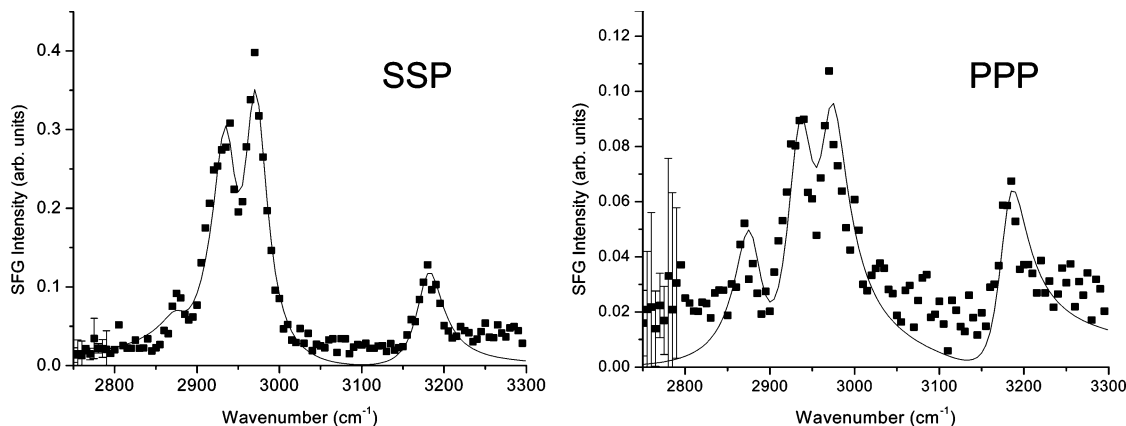
After taking into account the effects of Fermi resonance, instrumental efficiency, normalization of peak widths, and rigorous error analysis the intensity ratios can be compared with the theoretical curves as shown in Figures 8-10.

For each of the molecules studied orientation calculations were performed for H-C(4)C(5)-H vibrational modes from the ring, which are assumed to have  $C_{2v}$  symmetry, and the methyl group at the end of the butyl chain, which is assumed to have  $C_{3v}$  symmetry.

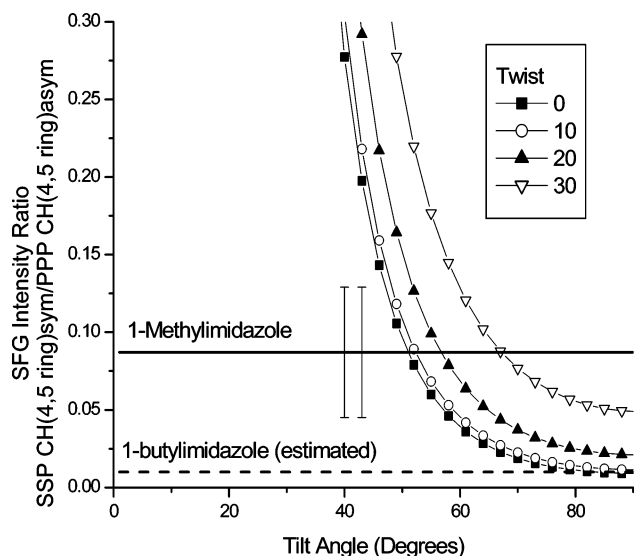
For determination of the orientation of the methyl groups of the two ionic liquids studied it was assumed that all intensity attributed to the peak at 2970  $\text{cm}^{-1}$  was from the asymmetric methyl stretch from the butyl chain, and no intensity from the symmetric N-CH<sub>3</sub> vibration. This estimation is based on Raman and infrared experiments performed on deuterated samples of the ionic liquids used.<sup>44</sup> In both the infrared and Raman spectra of the ionic liquids with deuterated alkyl chains the N-CH<sub>3</sub> vibrations were very weak. By comparing spectra with the alkyl chain or the N-CH<sub>3</sub> deuterated it was determined that the contribution from the N-CH<sub>3</sub> vibrations was negligible. SFG

TABLE 5: Peak Fitting Parameters from SFG Spectra Used in Orientation Calculation

	A ( $\Gamma$ )							
	1-methylimidazole		1-butylimidazole		[BMIM][BF <sub>4</sub> ]		[BMIM][PF <sub>6</sub> ]	
	ssp	ppp	ssp	ppp	ssp	ppp	ssp	ppp
symmetric CH <sub>3</sub>	15.2 (16.9)	3.33 (19.9)	-3.29 (10.8)	-4.50 (16.0)	1.40 (14.6)	2.04 (2T0.0)	1.07 (17.2)	3.43 (20.0)
Fermi resonance	8.60 (16.9)	1.24 (19.9)	-13.5 (20.0)	-4.50 (16.0)	5.03 (15.8)	3.69 (18.4)	6.55 (17.2)	4.65 (20.0)
antisymmetric CH <sub>3</sub>	8.49 (16.9)	8.79 (19.9)	12.9 (20.0)	-4.50 (16.0)	11.0 (15.8)	7.05 (18.4)	8.52 (17.2)	3.84 (20.0)
antisymmetric ring	17.5 (17.0)	14.9 (22.0)		1.00 (16.0)				
symmetric ring	3.18 (17.0)	3.53 (22.0)			4.55 (20.0)	4.90 (20.0)	6.67 (20.0)	4.29 (20.0)



**Figure 7.** SFG spectra of 1-butyl-3-methylimidazolium [PF<sub>6</sub>]/quartz interface w/fit.



**Figure 8.** Simulation of SFG signal as a function of ring mode orientation of the liquid/quartz interface.

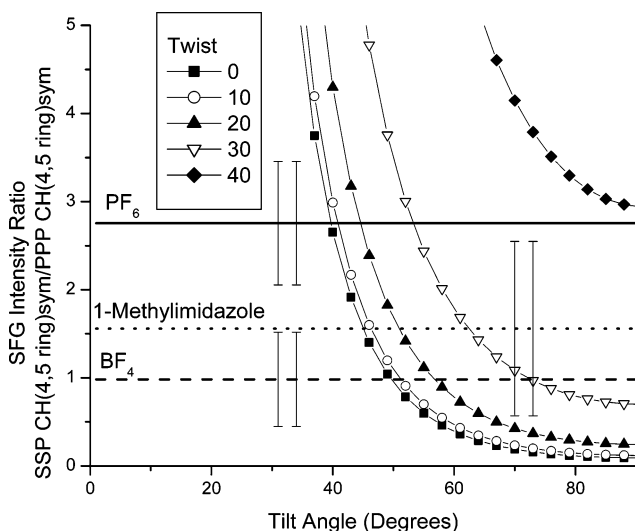


**Figure 9.** Simulation of SFG signal as a function of ring mode orientation of the liquid/quartz interface.

experiments of the air/liquid interface of deuterated [BMIM]-[BF<sub>4</sub>] and [BMIM][PF<sub>6</sub>] also show that the contribution from the methyl group attached to the nitrogen is much weaker than that for the methyl group at the end of the butyl chain.<sup>44</sup>

The orientation of the methyl group at the end of the butyl chain was also estimated for 1-butylimidazole, [BMIM][BF<sub>4</sub>],

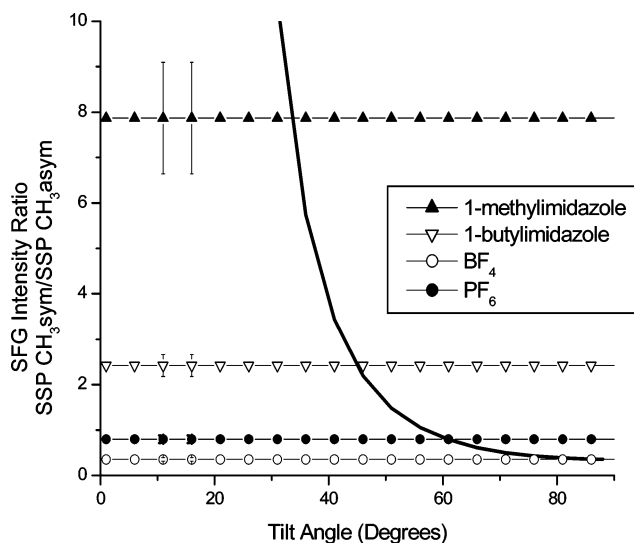


**Figure 10.** Simulation of SFG signal as a function of methyl group orientation of the liquid/quartz interface.

and [BMIM][PF<sub>6</sub>]. The reason an exact value was unable to be determined was that the peak assigned to the Fermi resonance of the methyl group contained more amplitude than the fundamental. This is likely due to the difficulty in fitting SFG spectra which could be from an unassigned vibration(s).

For both the ring and methyl orientation calculations of each of the molecules studied all possible intensity ratios and polarization combinations were examined and showed to be in agreement with each other. Therefore, only one of the possible intensity ratios is shown for each methyl and ring orientation for simplicity.

By determining the orientation of both the methyl group and the ring of the molecules studied a more complete picture of the overall orientation at the interface is presented.

**Model of Quartz Surface.** To make predictions of how the molecules studied in this paper are oriented at the interface a fundamental model of the quartz surface is explained herein. The fused quartz used in this experiment is expected to be covered with silanol groups because of the repeated washings after cleaning with 50/50 HNO<sub>3</sub>/H<sub>2</sub>SO<sub>4</sub>. The excess adsorbed water was then removed under vacuum before addition of the molecule under investigation. The amount of siloxane bonds on the surface should be small because the quartz was kept at room temperature. Because polar molecules adsorb at silanol groups, for maximum adsorption the silica surface should be free of adsorbed water and have a maximum concentration of silanol groups.<sup>59</sup> For nonaqueous solutions, hydrogen bond

formation between electronegative atoms or  $\pi$ -electrons of adsorbate molecules and hydrogen atoms of the silanol groups and the silica surface play a major role in adsorption.

**Orientation of the 1-Methylimidazole/Quartz Interface.** Comparison of the ring modes intensities from the H–C(4)C–(5)–H stretches is shown in Figures 8 and 9. Figure 8 predicts the tilt angle to be between 47° and 68° with the twist angle between 0° and 30°. Figure 9 predicts that the tilt angle for the ring is between 45° and 63° with the twist angle between 0° and 30°. When comparing the methyl stretches of 1-methylimidazole, Figure 10, it was determined that the methyl group had a tilt angle between 32° and 35°. 1-methylimidazole is expected to form weak hydrogen bonds between the nitrogen atoms of 1-methylimidazole and surface silanol OH groups, as has been reported for other molecules with similar structures.<sup>60,61</sup> Since the calculated twist angle of the ring is small, both nitrogens from the ring are believed to be undergoing some hydrogen bonding. In order for the orientation of the methyl group to correctly correlate with the ring orientation the ring must be slightly twisted. This suggests there is less hydrogen bonding with the nitrogen attached to the methyl group. The compact shape of 1-methylimidazole, as compared to the other molecules studied, allows for a more compressed packing at the quartz surface.

**Orientation of the 1-Butylimidazole/Quartz Interface.** SFG spectra of 1-butylimidazole show only one peak due to the H–C(4)C(5)–H stretches from the ring, therefore the orientation of the ring must be estimated. This estimation is due to the fact that a symmetric mode should be visible in the SFG spectra if the mode has some component in the  $z$  direction. Because the symmetric mode of the ring is not visible in either polarization combination, the tilt angle is suggested to be between 70° and 90°, nearly parallel to the surface, with the twist angle being nearly 0°. Figure 10 shows the value for the tilt angle of the methyl group to be around 43–47°. Comparison of the symmetric and asymmetric modes of the ssp spectra was chosen due to the greater signal-to-noise of the ssp spectra compared with the ppp spectra. The difference in orientation of the imidazole rings of 1-methylimidazole and 1-butylimidazole is believed to be due to the asymmetry of the 1-butylimidazole molecule. The hydrophobic character of the alkyl chain is believed to be influencing the orientation of the ring. 1-Methylimidazole is tilted up from the surface in comparison with 1-butylimidazole. This is probably due to the more symmetric shape of 1-methylimidazole, giving it more freedom to pack at the surface, as well as a larger relative contribution from hydrogen bonding of the nitrogen (compared to van der Waals forces of the alkyl chain).

**Orientation of the [BMIM][BF<sub>4</sub>]/Quartz Interface.** SFG spectra of [BMIM][BF<sub>4</sub>] only contain symmetric vibrations from the ring. Figure 9 shows the comparison of the intensities of the symmetric modes from the ring. The tilt angle of the ring is between 45° and 90°, with a possible twist angle of 0–30°. The orientation of the methyl group at the end of the butyl chain is calculated to be 78–90°, nearly parallel to the surface. As with both imidazole molecules, [BMIM][BF<sub>4</sub>] is believed to be hydrogen bonded to the quartz surface through both nitrogens on the ring. There is also the possibility that there are hydrogen bonding interactions with the  $\pi$  orbitals of the aromatic ring. The butyl chain is then expected to be nearly flat on the quartz surface due to van der Waals interactions between the quartz surface and the alkyl chain.

**Orientation of the [BMIM][PF<sub>6</sub>]/Quartz Interface.** The SFG spectra of [BMIM][PF<sub>6</sub>] ionic liquid are similar to those

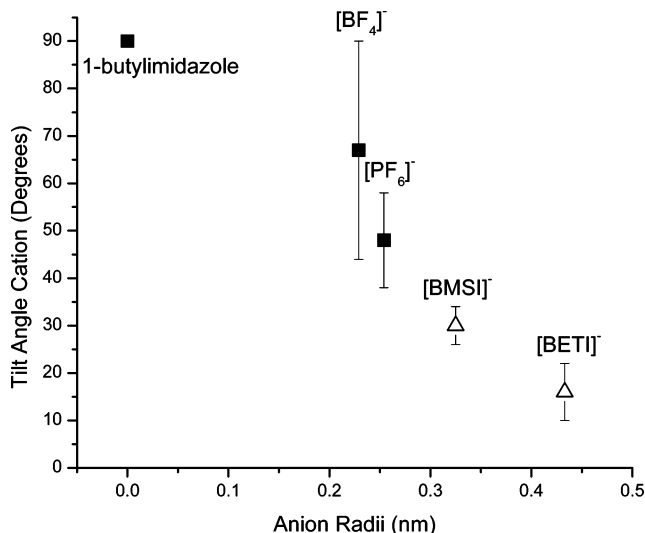


**Figure 11.** Tilt angle of the cation ring as a function of anion radius. Solid symbols are from this work. Open points are derived from Conboy et al.<sup>23</sup>

of [BMIM][BF<sub>4</sub>]. Only the symmetric modes from the H–C(4)C–(5)–H stretch of the ring are visible in the ssp and ppp spectra. Figure 9 predicts the orientation of the ring to have a tilt angle of 38–58° with a twist angle between 0° and 30°. The orientation of the methyl group at the end of the butyl chain is determined to be around 58–64° from Figure 10.

There are several possible reasons for the differences in orientation of the ring of the two ionic liquids studied. The size anion seems to be the more likely cause for the difference in orientation. The ring of 1-butylimidazole lies parallel with the surface while the rings of the two ionic liquids are tilted upward. This may be due to the change in the unit cell of each of the molecules studied. The only other study investigating the orientation of ionic liquids at a quartz interface was performed by Conboy et al.<sup>23</sup> The anions used in that study were imide based and were very hydrophobic and much larger. In that study the orientation of the imidazolium rings was determined to have a tilt angle between 16° and 32° from normal. Comparing the results of this study with those of Conboy's study shows that as the size of the anion is increased the orientation of the cation is tilted upward toward normal. This leads to the conclusion that the orientation of the cation is influenced by the size of the anion. The sizes of the ionic radii are as follows: 0.229 nm for tetrafluoroborate, 0.254 nm for hexafluorophosphate, 0.325 nm for bis(trifluoromethylsulfonyl)imide (BMSI), and 0.433 nm for bis(perfluoroethylsulfonyl)imide (BETI).<sup>23</sup> The radius of BETI was calculated by comparing the value published for BMSI with calculations performed in PC Spartan for BMSI and BETI. Figure 11 shows a plot of the tilt angle of the cation ring versus the radius of the anion. The figure shows that as the anion size is increased the tilt of the cation is projected more toward the normal. 1-Butylimidazole is a neutral molecule and lies flat on the quartz surface because it is not influenced by an anion. The hexafluorophosphate ion is 10% larger than the tetrafluoroborate ion causing the ring of the cation to tilt more toward normal. The imide-based anions used in Conboy's study were 40% (BMSI) and 90% (BETI) larger than the tetrafluoroborate anion, respectively, which corresponds well with the ring being tilted much closer to normal in Conboy's study. The anion is attracted to the cation through Coulombic forces and must therefore be within a certain distance from the cation. This allows for the ability to make some statements about the position of the anion. Inorganic salts that are soluble in organic solvents

are known to adsorb to silica surfaces.<sup>59,62</sup> Because the cation's orientation is affected by the size of the anion, this suggests that the anion is positioned next to the cation adsorbed to the quartz surface.

The study of ionic liquids provides an opportunity to study double-layer effects at extremely high concentrations of electrolyte. Because the quartz surface is neutral, both the cation and anion adsorb to the surface in order to keep the charge balanced. As the size of the anion is increased the cation is tilted more toward normal, because of the Coulombic interaction, to keep the same amount of charged species in contact with the quartz surface. The structure of the interface is believed to be described by a competition of two competing forces: attraction due to van der Waals forces and an electrical double-layer repulsion. These effects are described by Derjaguin–Landau–Verwey–Overbeek (DLVO) theory for low electrolyte solutions but the same forces are apparent for solutions with high concentrations of electrolyte.<sup>63,64</sup>

The difference in the orientation of the methyl group from the butyl chain of the studied molecules is believed to be from the change in orientation of the ring. It is difficult to make direct comparisons with Conboy's study because the imidazolium based ionic liquids used in that study have longer chain lengths. The methyl groups are oriented more toward normal in Conboy's studies, which is expected for ionic liquids with larger anions.

This work has examined how two imidazolium based ionic liquids and two similar uncharged species orient at a quartz surface and compared these results with a previous study of a different ionic liquid. Ionic liquids are composed of only charged species, therefore, how these species orient on surfaces can directly affect their properties. Understanding the double-layer structure of ionic liquids is still in its infancy, and the conclusion that both the cation and anion are adsorbed to the quartz surface will hopefully lead to a clearer model. Silica substrates are used as support material used for supported ionic liquid heterogeneous catalysis.<sup>65</sup> A better understanding of the double-layer structure would be highly beneficial for the design of heterogeneous catalysis with ionic liquids. Because the physical properties of ionic liquids can be "tuned" by changing the cation or anion, a solid understanding of how these changes affect the quartz/ionic liquids interface is applicable for several industrial applications: such as lubrication, chromatography, and solar cells.

## Conclusions

SFG spectroscopy was used to characterize the interfacial properties of two ionic liquids as well as 1-methylimidazole and 1-butylimidazole on a quartz surface. Raman spectroscopy was used to identify vibrations and conclude whether they were symmetric or asymmetric. It was determined that the 1-methylimidazole ring has a tilt angle between 45° and 68° with a twist angle between 0° and 30°. 1-Butylimidazole lies flat in the plane of the interface with the methyl group at the end of the butyl chain having a tilt angle between 43° and 47°. The tilt angle of the [BMIM][BF<sub>4</sub>] ionic liquid imidazolium ring was determined to be 45–90° with a twist angle between 0° and 30°. The methyl group at the end of the butyl chain has a tilt angle of 78–90°. The imidazolium ring of the [BMIM][PF<sub>6</sub>] ionic liquid was tilted more toward normal, 38–58°, with a twist angle between 0° and 30°. The methyl group was also tilted more toward normal, 58–64°. It was concluded that the larger the anion the more the imidazolium ring is tilted toward normal. The influence of the anion on the cation's orientation suggests

that the anion is also in contact with the quartz surface and *not* positioned above or below the cation in a double layer-type structure.

**Acknowledgment.** This work was supported by grants from the Robert A. Welch Foundation, United States Air Force, and Universal Energy Systems. The authors thank Adelajda Zereba and Roman Czernuszewicz for their help in acquiring depolarized Raman spectra.

## References and Notes

- (1) Seddon, K. R. *J. Chem. Technol. Biotechnol.* **1997**, *68*, 351.
- (2) Wasserscheid, P.; Keim, W. *Angew. Chem., Int. Ed.* **2000**, *39*, 3772.
- (3) Sheldon, R. *Chem. Commun.* **2001**, 2399.
- (4) Dupont, J.; Souza, R. F.; Suarez, P. A. *Chem. Rev.* **2002**, *102*, 3667.
- (5) Rogers, R. D.; Huddleston, J. G.; Williauer, H. D.; Swatloski, R. P.; Visser, A. E. *Chem. Commun.* **1998**, 1765.
- (6) Abraham, M. H.; Zissimos, A. M.; Huddleston, J. G.; Willauer, H. D.; Rogers, R. D.; Acree, W. E. *Ind. Eng. Chem. Res.* **2003**, *42*, 413.
- (7) Wang, P.; Zakeeruddin, S. M.; Moser, J. E.; Gratzel, M. *J. Phys. Chem. B* **2003**, *107*, 13280.
- (8) Papageorgiou, N.; Athanassov, Y.; Armand, M.; Bonhote, P.; Pettersson, H.; Azam, A.; Gratzel, M. *J. Electrochem. Soc.* **1996**, *143*, 3099.
- (9) Phillips, B. S.; Zabinski, J. S. *Tribol. Lett.* **2004**, *17*, 533.
- (10) Ye, C.; Liu, W.; Chen, Y.; Ou, Z. *Wear* **2002**, *253*, 579.
- (11) Omotowa, B. A.; Phillips, B. S.; Zabinski, J. S.; Shreeve, J. M. *Inorg. Chem.* **2004**, *43*, 5466.
- (12) Wang, H.; Lu, Q.; Ye, C.; Liu, W.; Cui, Z. *Wear* **2004**, *256*, 44.
- (13) Lu, Q.; Wang, H.; Ye, C.; Liu, W.; Xue, Q. *Tribol. Int.* **2004**, *37*, 547.
- (14) Iimori, T.; Iwahashi, T.; Ishii, H.; Seki, K.; Ouchi, Y.; Ozawa, R.; Hamaguchi, H.; Kim, D. *Chem. Phys. Lett.* **2004**, *389*, 321.
- (15) Baldelli, S. *J. Phys. Chem. B* **2003**, *107*, 6148.
- (16) Rivera-Rubero, S.; Baldelli, S. *J. Phys. Chem. B* **2004**, *108*, 15133.
- (17) Rivera-Rubero, S.; Baldelli, S. *J. Am. Chem. Soc.* **2004**, *126*, 11788.
- (18) Solutskin, E.; Ocko, B. M.; Taman, L.; Kuzmenko, I.; Gog, T.; Deutsch, M. *J. Am. Chem. Soc.* **2005**, *127*, 7796.
- (19) Watson, P. R.; Gannon, T. J.; Law, G.; Carmichael, A. J.; Seddon, K. R. *Langmuir* **1999**, *15*, 8429.
- (20) Watson, P. R.; Law, G. *Chem. Phys. Lett.* **2001**, *345*, 1.
- (21) Katayanagi, H.; Hayashi, S.; Hamaguchi, H.; Nishikawa, K. *Chem. Phys. Lett.* **2004**, *392*, 460.
- (22) Bowers, J.; Vergara, M. C.; Webster, J. R. P. *Langmuir* **2004**, *20*, 309.
- (23) Fitchett, B. D.; Conboy, J. C. *J. Phys. Chem. B* **2004**, *108*, 20255.
- (24) Feller, M. B.; Chen, W.; Shen, Y. R. *Phys. Rev. A* **1991**, *43*, 6778.
- (25) Miranda, P. B.; Shen, Y. R. *J. Phys. Chem. B* **1999**, *103*, 3292.
- (26) Wei, X.; Hong, S.; Zhuang, X.; Shen, Y. R. Personal communication, 2000.
- (27) Bell, G. R.; Bain, C. D.; Ward, R. N. *J. Chem. Soc., Faraday Trans.* **1996**, *92*, 515.
- (28) Hirose, C.; Akamatsu, N.; Domen, K. *Appl. Spectrosc.* **1992**, *46*, 1051.
- (29) Long, D. A. *Raman Spectroscopy*; McGraw-Hill: New York, 1977.
- (30) Nakamoto, K. *Infrared and Raman Spectra of Inorganic and Coordination Compounds*; John Wiley & Sons: New York, 1997.
- (31) Czernuszewicz, R. S. Resonance Raman Spectroscopy of Metalloproteins using CW Laser Excitation. In *Methods in Molecular Biology: Spectroscopic Methods and Analyses: NMR, Mass Spectrometry, and Metalloprotein Techniques*; Jones, C., Mulloy, B., Thomas, A. H., Eds.; Humana Press: Totowa, NJ, 1993; Vol. 17.
- (32) *Handbook of Raman Spectroscopy*; Lewis, I. R., Edwards, H., Eds.; Marcel Dekker: New York, 2001.
- (33) Garfinkel, D.; Edsall, J. T. *J. Am. Chem. Soc.* **1958**, *80*, 3807.
- (34) Van Bael, M. K.; Smets, J.; Schoone, K.; Houben, L.; McCarthy, W.; Adamowicz, L.; Nowak, M. J.; Maes, G. *J. Phys. Chem. A* **1997**, *101*, 2397.
- (35) Tataru, W.; Wojcik, M. J.; Lindgren, J.; Probst, M. *J. Phys. Chem. A* **2003**, *107*, 7827.
- (36) Cao, P.; Gu, R.; Tian, Z. *J. Phys. Chem. B* **2003**, *107*, 769.
- (37) Carter, D. A.; Pemberton, J. E. *Langmuir* **1992**, *8*, 1218.
- (38) Carter, D. A.; Pemberton, J. E. *J. Raman Spectrosc.* **1997**, *28*, 939.
- (39) Perchard, C.; Novak, A. *Spectrochim. Acta A* **1967**, *23*, 1953.
- (40) Herzberg, G. *Molecular spectra and molecular structure*; D. Van Nostrand Company: New York, 1945.
- (41) Himmelhaus, M.; Disert, F.; Buck, M.; Grunze, M. *J. Phys. Chem.* **2000**, *104*, 576.
- (42) MacPhail, R. A.; Strauss, H. L.; Elliger, C. A.; Snyder, R. G. *J. Phys. Chem.* **1984**, *88*, 334.

- (43) Talaty, E. R.; Raja, S.; Strohaug, V. J.; Dolle, A.; Carper, W. R. *J. Phys. Chem. B* **2004**, *108*, 13177.
- (44) Rivera-Rubero, S.; Baldelli, S. Submitted for publication.
- (45) Dieter, K. M.; Dymek, C. J.; Heimer, N. E.; Rovang, J. W.; Wilkes, J. S. *J. Am. Chem. Soc.* **1988**, *110*, 2722.
- (46) Lobau, J.; Wolfrum, K. *J. Opt. Soc. Am. B* **1997**, *14*, 2505.
- (47) Carmichael, A. J.; Hardacre, C.; Holbrey, J. D.; Seddon, K. R.; Nieuwenhuyzen, M. *Proc. Electrochem. Soc.* **XXXX**, 99–41, 209.
- (48) Dymek, C. J.; Stewart, J. P. *Inorg. Chem.* **1989**, *28*, 1472.
- (49) Weast, R. C. *CRC Handbook of Chemistry and Physics*; CRC Press: Cleveland, OH, 1984.
- (50) Dean, J. A. *Lange's handbook of Chemistry*; McGraw-Hill: New York, 1992.
- (51) Zhuang, X.; Miranda, P. B.; Kim, D.; Shen, Y. R. *Phys. Rev. B* **1999**, *59*, 12632.
- (52) Braun, R.; Casson, B. D.; Bain, C. D. *J. Chem. Phys.* **1999**, *110*, 4634.
- (53) Hirose, C.; Akamatsu, N.; Domen, K. *J. Chem. Phys.* **1992**, *96*, 997.
- (54) Wilson, E. B.; Decius, J. C.; Cross, P. C. *Molecular vibrations*; McGraw-Hill: New York, 1955.
- (55) Bunker, P. R. *Molecular symmetry and spectroscopy*; Academic: New York, 1970.
- (56) Demtroder, W. *Laser Spectroscopy*; Springer: New York, 1996.
- (57) McHale, J. L. *Molecular Spectroscopy*; Prentice Hall: Upper Saddle River, NJ, 1999.
- (58) Skoog, D. A.; Holler, F. J.; Nieman, T. A. *Principles of Instrumental Analysis*, 5th ed.; Saunders College: Fort Worth, TX, 1998.
- (59) Iler, R. K. *The Chemistry of Silica*; John Wiley & Sons: New York, 1979.
- (60) Liu, D.; Ma, G.; Allen, H. C. *Environ. Sci. Technol.* **2005**, *39*, 2025.
- (61) Dines, T. J.; MacGregor, L. D.; Rochester, C. H. *Spectrochim. Acta A* **2003**, *59*, 3205.
- (62) Maatman, R.; Geertsema, A.; Verhage, H.; Baas, G.; Du Mez, M. *J. Chem. Phys.* **1968**, *72*, 97.
- (63) Horn, R. G.; Evans, D. F.; Ninham, B. W. *J. Phys. Chem.* **1988**, *92*, 3531.
- (64) Israelachvili, J. N.; Adams, G. E. *J. Chem. Soc., Faraday Trans.* **1978**, *74*, 975.
- (65) Mehnert, C. P.; Cook, R. A.; Dispenziere, N. C.; Afeworki, M. *J. Am. Chem. Soc.* **2002**, *124*, 12932.